HHS Public Access

Author manuscript

Prostate. Author manuscript; available in PMC 2021 February 01.

Published in final edited form as:

Prostate. 2020 August ; 80(11): 872–884. doi:10.1002/pros.24020.

Urethral luminal epithelia are castration-insensitive cells of the proximal prostate

Diya B. Joseph, PhD[1], **Gervaise H. Henry, MS**[1,2], **Alicia Malewska, MS**[1], **Nida S. Iqbal, PhD**[1], **Hannah M. Ruetten**[3], **Anne E. Turco**[3], **Lisa L. Abler, PhD**[3], **Simran K. Sandhu**[3], **Mark T. Cadena**[3], **Venkat S. Malladi, MS**[2], **Jeffrey C. Reese, MD**[4], **Ryan J. Mauck, MD**[1], **Jeffrey C. Gahan, MD**[1], **Ryan C. Hutchinson, MD**[1], **Claus G. Roehrborn, MD**[1], **Linda A. Baker, MD**[1], **Chad M. Vezina, PhD**[3], **Douglas W. Strand, PhD**[1]

[1]Department of Urology, UT Southwestern Medical Center, Dallas, Texas

[2]Department of Bioinformatics, UT Southwestern Medical Center, Dallas, Texas

[3]Department of Comparative Biosciences, School of Veterinary Medicine, University of Wisconsin-Madison, Madison, Wisconsin

[4]Southwest Transplant Alliance, Dallas, Texas

Abstract

Background: Castration-insensitive epithelial progenitors capable of regenerating the prostate have been proposed to be concentrated in the proximal region based on facultative assays. Functional characterization of prostate epithelial populations isolated with individual cell surface markers has failed to provide a consensus on the anatomical and transcriptional identity of proximal prostate progenitors.

Methods: Here, we use single-cell RNA sequencing to obtain a complete transcriptomic profile of all epithelial cells in the mouse prostate and urethra to objectively identify cellular subtypes. Pan-transcriptomic comparison to human prostate cell types identified a mouse equivalent of human urethral luminal cells, which highly expressed putative prostate progenitor markers. Validation of the urethral luminal cell cluster was performed using immunostaining and flow cytometry.

Results: Our data reveal that previously identified facultative progenitors marked by Trop2, Sca-1, KRT4, and PSCA are actually luminal epithelial cells of the urethra that extend into the proximal region of the prostate, and are resistant to castration-induced androgen deprivation. Mouse urethral luminal cells were identified to be the equivalent of previously identified human club and hillock cells that similarly extend into proximal prostate ducts. Benign prostatic hyperplasia (BPH) has long been considered an “embryonic reawakening,” but the cellular origin

Correspondence: Douglas W. Strand, PhD, Department of Urology, UT Southwestern Medical Center, Dallas, TX 75390. Douglas.Strand@UTSouthwestern.edu.

CONFLICT OF INTERESTS

The authors declare that there are no conflict of interests.

SUPPORTING INFORMATION

Additional supporting information may be found online in the Supporting Information section.

of the hyperplastic growth concentrated in the periurethral region is unclear. We demonstrate an increase in urethral luminal cells within glandular nodules from BPH patients. Urethral luminal cells are further increased in patients treated with a 5-α reductase inhibitor.

Conclusions: Our data demonstrate that cells of the proximal prostate that express putative progenitor markers, and are enriched by castration in the proximal prostate, are urethral luminal cells and that these cells may play an important role in the etiology of human BPH.

Keywords

benign prostatic hyperplasia; castration; prostate stem cell; prostatic urethra; single-cell RNA sequencing

1 | INTRODUCTION

The mouse and human prostate develop as a series of solid epithelial buds from the primitive urethra, or urogenital sinus. Buds undergo a period of branching morphogenesis and canalization resulting in a tree-like network of proximal ducts and distal glands.[1–3] We previously produced a cellular atlas of the normal adult human prostate and prostatic urethra using single-cell RNA sequencing (scRNA-seq) on proximal and distal anatomical regions. These data confirmed known cell types of the prostate such as basal, luminal, and neuroendocrine cells, and led to the identification of previously unknown hillock and club cells as the major luminal epithelial cell types comprising the prostatic urethra and its proximal ducts.[4] Studies in other organs have shown that a rigorous mapping of equivalent mouse cell types with objectively defined cell type-specific markers can lead to better models of human disease,[5,6] but a similar comparative cellular atlas of the human and mouse prostate has not been compiled.

The human prostate consists of a network of 12 to 14 paired proximal ducts that empty secretory products of distal glandular units into the urethra.[7] Benign prostatic hyperplasia (BPH) is an expansion of the periurethral transition zone surrounding the urethra that occurs in a majority of aging men and is commonly treated with 5-α reductase inhibitors (5ARIs) that cause apoptosis of androgen-dependent prostate luminal cells.[8,9] The cellular origin of periurethral prostate growth is unknown, but has been hypothesized to be mediated through a reawakening of embryonic growth signaling.[10–13]

During early postnatal development, multipotent basal epithelial progenitors located throughout the prostate give rise to basal, luminal, and neuroendocrine cell types.[14,15] At puberty these multipotent basal cells become restricted to distal tips, which were shown previously to be the main site of proliferation during androgen-induced regenerative growth after castration.[16] In the adult, basal and luminal lineages are maintained by unipotent progenitors,[17] but an “intermediate” cell type with both basal and luminal characteristics can give rise to luminal cells as well.[14] The prostate displays potent regenerative capacity after castration and subsequent androgen replenishment,[18] prompting the search for castration-insensitive prostate progenitors. Lineage tracing of Keratin 8-expressing luminal epithelia demonstrates that prostate luminal cells are largely derived from unipotent luminal progenitors after castration and regeneration.[17,19,20] Several studies have identified cell

populations characterized by expression of Sca-1,[21,22] Trop2,[23] LY6D,[24] and KRT4[19,25] that are enriched in the proximal region of the mouse prostate after castration, form spheroids at high frequency, and can act as facultative progenitors in prostate regeneration assays. A proximal to distal expansion of progenitors has been demonstrated in human lineage tracing studies.[26,27] Proximal epithelial cells purified with individual cell surface markers show progenitor activity,[21,28–30] but these cell surface markers are expressed across multiple tissue types, making it difficult to precisely capture the identity of cell types of interest. These issues exemplify the need for objective transcriptional identities of each cell type in the prostate and urethra to build lineage tracer mouse models capable of selectively marking specific cell types.

Cell identity has historically been defined by a small combination of markers, and the interpretation of data from experimental mouse models relies on these definitions. Here, we use scRNA-seq of the mouse prostate and urethra to build a comparative cellular atlas to the human to bolster the molecular and anatomical definition of each epithelial cell type.[4,31] We use scRNA-seq, flow cytometry, and immunohistochemistry to demonstrate that proximal castration-insensitive cells expressing progenitor markers correspond to a urethral luminal epithelial cell type that exists in the urogenital sinus during prostate budding, and extends into the ductal network of the proximal prostate in the normal adult. Urethral luminal cells are increased in the proximal prostate of castrated mice as well as in human BPH patients treated with a 5ARI. When comparing the transcriptome of urethral luminal epithelia in normal adults to BPH patients, an increase in immunomodulatory gene expression is observed. In summary, our data demonstrate that castration-insensitive cells expressing progenitor markers in the proximal prostate are actually an extension of the immunomodulatory urethral luminal epithelia and that this cell type is resistant to 5ARI treatment in human BPH.

2 | MATERIALS AND METHODS

2.1 | Human subjects

Healthy prostate specimens used in this study were obtained from fifteen, 17- to 42-year-old male organ donors whose families were consented at the Southwest Transplant Alliance from March 2017 to January 2020 under IRB STU 112014–033. BPH specimens were obtained fresh from 28 patients undergoing simple prostatectomy at UT Southwestern Medical Center. Fetal lower urinary tracts were obtained from the University of Pittsburgh Medical Center and Joint MRC/Wellcome (MR/R006237/1) Human Developmental Biology Resource (www.hdbr.org) under an approved University of Wisconsin-Madison IRB protocol (2016–137 0449). Clinical details for each fetal, normal adult, and diseased adult human specimen and their usage in associated figures are shown in Table S1.

2.2 | Mouse tissue collection and castration

Animal work described in this manuscript has been approved and conducted under the oversight of the UT Southwestern Institutional Animal Care and Use Committee. Male C57BL/6 mice (8–12 weeks) were obtained from the UT Southwestern Mouse Breeding Core. Lower urinary tract tissues were collected from mice after euthanasia. Eleven-week-

old mice were subjected to castration surgery following approved surgery protocols. The prostate was allowed to involute for 2 weeks before the mice were euthanized for tissue collection.

2.3 | Tissue processing

Fresh tissue samples were transported in ice-cold saline and immediately dissected into portions for fixation in 10% formalin followed by paraffin embedding. For human specimens, a 4-hour enzymatic digestion into single cells was performed at 37°C in 35 mL Hanks' balanced salt solution (HBSS) containing 5 mg/mL Collagenase Type I (Life Technologies), 10 μM ROCK Inhibitor Y-27632 (StemRD), 1 nM dihydrotestosterone (DHT) (Sigma-Aldrich), 1 mg DNAse I (Roche), and 1% antibiotic/antimycotic solution (100×; Corning).[4] Mouse specimens were digested for 1 hour in HBSS containing either 10 mg/mL cold protease or 1.5 to 2 mg/mL Collagenase Type I, plus 10 μM ROCK Inhibitor Y-27632, 1 nM DHT, 1 mg DNAse I, and 1% antibiotic/antimycotic solution.

2.4 | Flow cytometry

Human and mouse prostate and urethral cells were analyzed at the UT Southwestern CRI Flow Cytometry Core on a BD FACSAria Fusion SORP or a BD FACSAria II SORP 5-laser flow cytometer and analyzed with FlowJo software as previously published.[4] Prostate stem cell antigen-positive (PSCA)+ urethral cell counts from normal and BPH prostates were tested for differences using Student's *t* test. Improved antibody panels based on single-cell data were built with fluorescence minus one experiments. Table S2 displays information on antibodies used for flow cytometry.

2.5 | Immunohistochemistry

In brief, 5-μm paraffin sections were deparaffinized in xylene and hydrated through a series of ethanol washes. To block endogenous peroxidases, tissues were blocked with 0.3% H_2O_2 in methanol for 20 minutes. Following a wash in phosphate-buffered saline (PBS), heat-mediated antigen retrieval was performed by boiling slides in Vector Antigen Unmasking Solution (H-3300; Vector Labs) for 20 minutes in a conventional microwave oven. Tissues were blocked with 2.5% Horse Serum (Vector Labs) for 20 minutes. For the first stage of staining, the first primary antibody diluted in 2.5% Horse Serum was applied for 1 hour at room temperature. Following washes in PBS, tissues were incubated with enzyme-conjugated secondary antibody solution for 30 minutes at room temperature. Tissues were washed twice in PBS and substrate solution was added to develop antibody stain. This was repeated for the second primary antibody. Horseradish peroxidase and alkaline phosphatase enzyme systems from Vector Laboratories were used to obtain dual stains. Tissues were counterstained with hematoxylin and mounted with permount solution. For primary and secondary antibody information see Table S2.

2.6 | Immunofluorescence

Five-micrometer paraffin sections were deparaffinized in xylene and hydrated through a series of ethanol washes. Heat-mediated antigen retrieval was performed by boiling slides in Vector Antigen Unmasking Solution (H-3300) for 20 minutes in a conventional microwave

oven. Tissues were washed with PBS and nonspecific binding sites were blocked for 1 hour in blocking buffer (1× Tris-buffered saline, 5% normal horse serum, 0.1% bovine serum albumin, 0.1% Tween-20, 0.2 mM sodium azide). Tissues were incubated overnight at 4°C with primary antibodies diluted in blocking buffer. Tissues were washed several times in PBS and incubated with secondary antibodies diluted in blocking buffer for 1 hour at room temperature. Following several washes with PBS, tissues sections were incubated with 4′,6-diamidino-2-phenylindole, dilactate (DAPI) to visualize cell nuclei and mounted with PBS containing 90% glycerol and 0.2% *n*-propyl gallate. Images were obtained using a Nikon Eclipse Ti-U with NIS-Elements software or a Zeiss Axioscan Z1 microscope.

2.7 | Cell counting

Cell counting was performed using the Cell Counter plugin in ImageJ (Fiji) 2.0.0. Cell counts were obtained across different anatomical regions (ducts/prostate, urogenital sinus/prostate buds, urethra/ proximal ducts/distal prostate) and expressed as counts/total cells counted or presented as mean percentage ± standard error of the mean.

2.8 | Stain quantification

Quantification of SCGB1A1 and KRT13 antibody staining was performed using ImageJ (Fiji) 2.0.0. Color deconvolution was performed to isolate SCGB1A1 stain (brown), KRT13 stain (red), and nuclei (blue). Thresholding was performed to isolate positive pixels. Area of positively stained pixels was divided by total pixel area of the tissue section.

2.9 | Statistical analysis

Statistical analyses were conducted with R version 3.5.2. Homogeneity of variance was determined using Bartlett's test package for R. Student's *t* test was performed on parametric data with two independent groups. The Mann-Whitney *U*/the Wilcoxon rank sum test was performed on nonparametric data with two independent groups. $P < .05$ were considered statistically significant.

2.10 | Single-cell sequencing

Four mouse prostates and three mouse urethra samples were used for single-cell sequencing. In addition, three young human prostate specimens used previously[4,32] were sequenced deeper (Table S3). Single-cell analysis was performed as described previously[4,32] with additional modifications detailed in the Supporting Information Data. The code used to perform the analysis is publicly available.[33]

2.11 | Data and software availability

Data generated as part of this study were deposited into the GUDMAP consortium database and are fully accessible at https://doi.org/10.25548/16-WM8C.[34]The scRNA-seq data was deposited into GEO GSE145843 (human normal), GSE145838 (human BPH), GSE145861 (prostate) and GSE145865 (urethra). R code used to produce all the scRNA analysis is publicly available.[33] Analyzed scRNA-seq data from mouse and human specimens can be found at http://strandlab.net/sc.data/, where gene expression can be investigated in the cell type clusters identified in this study.

3 | RESULTS

3.1 | Identification of equivalent epithelial cell types of the prostate and urethra in the mouse vs human

We set out to identify equivalent mouse and human epithelial cell types in the prostate and urethra by scRNA-seq, given the widespread use of the mouse in modeling human prostate disease. First, we combined ventral, dorsolateral, and anterior mouse prostate lobes for digestion and barcoding in aggregate. We also independently barcoded cells from the dissected urethra, which contains prostate-draining ducts, ejaculatory ducts, and the epithelium of the prostatic urethra enclosed by the skeletal muscle of the rhabdosphincter (Table S3). The data from the prostate and urethral regions were aggregated (Figure S1A) and equivalent cell types were identified by comparison to our previously published human prostate and urethra scRNA-seq data set.[4] First, major cell lineages (leukocytes, endothelia, fibromuscular stroma, and epithelia) in the mouse data were identified using the human scRNA-seq data (Figure S1A,B). Following this, the epithelia were subclustered and epithelial lineages were identified by comparison to human single-cell data (Figure S1C,D).

Epithelial clusters were displayed split by anatomical region into prostate and urethra (Figure 1A,B). Mouse epithelial cell clusters were defined based on the correlation to basal, luminal, and urethral luminal epithelia in humans[4] and included one basal, two urethral, and three luminal epithelial clusters (Figure 1C). Gene expression in the mouse basal cell cluster was highly correlated with the human basal cell cluster and enriched for *Krt5* and *Tp63* transcripts (Figures 1D and S1D). The three clusters of luminal epithelia corresponded to specific prostate lobes based on a previous study that identified lobe-specific gene expression of *Msmb* (dorsolateral, DLP), *Tgm4* (anterior, AP), and *Sbp* (ventral, VP) (Figure 1D).[35] Given the enrichment of the seminal vesicle-specific gene *Svs2*,[36] we labeled one of the urethral clusters as seminal vesicle and ejaculatory duct luminal cells (SV/ED luminal) (Figure 1D).

The other urethral cell cluster was found to correspond to the luminal epithelial cells of the prostatic urethra. The mouse urethral luminal epithelial cell type was identified based on correlation to human urethral luminal cell types (Figure 1C). Mouse urethral cells highly express Keratin 4 (Figure 1D) and are enriched in the urethra single-cell preparation compared with the prostate (Figure 1A vs 1B).

In the human prostate, club-type urethral cells are enriched in the urethral epithelium and proximal prostate ducts (Figure S2A). We were not able to identify a conventional club urethral epithelial cell type (characterized by expression of secretoglobins) in the mouse, either in the scRNA-seq data or by immunostaining (Figure S2B,C). However, mouse urethral luminal cells share several differentially expressed genes (DEGs) with human urethral cells, demonstrating the robustness of the transcriptomic correlation (Figure S2D and Table S4).[4] Figure 1D demonstrates the enrichment of DEGs for each mouse epithelial cluster. The full list of significant DEGs expressed in discrete cell types of the mouse prostate and urethra can be found in Table S5.

Similar to our previous human prostate study,[4] neuroendocrine epithelia are an extremely rare cell type that do not cluster independently, but can be identified using known markers such as CGRP and CHGA (Figure S3A,C). We also observed that neuroendocrine cells are enriched within the urethra and proximal prostatic ducts in the mouse and human (Figure S3B,D).

3.2 | Urethral luminal cells extend into the proximal ducts of the prostate and express markers of putative prostate progenitors and intermediate cells

Proximal ducts of the mouse prostate have been shown to contain a concentration of androgen-independent progenitors,[21,28–30] but identification of these cells has relied on a limited understanding of the expression of cell surface markers across all cell types. To determine precisely where urethral luminal cells are located, we performed immunofluorescent staining on transverse whole-mount sections of the mouse prostatic urethra with antibodies to KRT4 (urethral luminal cells), KRT5 (basal epithelia of urethra and prostate), and NKX3.1 (secretory prostate luminal cells).[37] We observed that luminal epithelia of the urethra and proximal ducts within and leading out of the rhabdosphincter are KRT4+/NKX3.1− and transition immediately into KRT4−/NKX3.1+ secretory prostate luminal cells (Figure 2A). The transition from urethral identity to prostate identity in human proximal ducts can be similarly highlighted using KRT13 (urethral luminal cells) and ACPP (prostate secretory luminal cells) (Figure 2B). At the pan-transcriptomic level, mouse urethral luminal cells have the highest correlation with human urethral cells (club and hillock) (Figure 1C). We conclude that these cells are luminal based on their cellular location in the suprabasal layers of the mouse urethral and proximal ductal epithelium (Figure 2A). Urethral luminal cells are a distinct population from the secretory prostate luminal epithelium, which express the prostate differentiation markers *Nkx3.1* and *Dpp4* (CD26) (Figure S4A). Furthermore, cell counts from the urethra, proximal ducts, and distal prostate demonstrate that KRT4+ cells do not coexpress NKX3.1 (Figure S4B). Similarly, KRT13+ cells do not co-express the secretory prostate luminal marker ACPP (Figure S4C). The transition from urethral luminal cells to secretory prostate luminal epithelium is clearly visible in the mouse and human periurethral “transition zone” (Figure 2A,B).

According to previous studies, prostate epithelia that are enriched in facultative stem cell assays display markers such as Sca-1 (LY6A),[21,22] Trop2 (TACSTD2),[23] LY6D,[24] and KRT4.[25,38] A dot plot of putative progenitor cell markers demonstrates that these genes are highly expressed in the urethral luminal epithelial cluster, although some proposed progenitor cell markers such as CD133 (*Prom1*) are enriched in luminal cells of the seminal vesicle and ejaculatory ducts (Figure 2C).[39] *Krt19* expression, which has been associated with KRT5+/KRT8+ “intermediate” cells transitioning from basal to luminal,[40] is highly enriched in urethral luminal epithelia (Figure 2C). Antibodies to CD49f and Sca-1 are commonly used to isolate prostate basal (CD49f^{hi}/Sca-1^{hi}) and luminal (CD49f^{lo}/Sca-1^{lo}) epithelia by flow cytometry.[23,25,30] Multiple studies have also identified a progenitor “LSC^{med}” population (CD49f^{med}/Sca-1^{hi}) enriched in castration and prostate tumor models.[21,25] Correlation analysis of transcriptomic signatures from cells in each of these three flow cytometry gates from Sackmann Sala et al[25] vs each of our scRNA-seq epithelial clusters demonstrates that the urethral luminal cell cluster is highly similar to the LSC^{med} androgen-

independent luminal progenitor (Figures 2D and S4D). These data suggest that the full identity of the castration-resistant putative prostate progenitor located in the proximal prostate is actually the urethral luminal cell.

3.3 | Trop2+ urethral luminal epithelia are enriched in the prostate after castration

Given the transcriptional similarity of urethral luminal epithelia to facultative progenitors (Figure 2C,D), we quantified the frequency of urethral luminal cells in discrete anatomical regions of the intact mouse prostate. We dissected the urethra away from proximal and distal prostate regions for digestion into single cells (Figure 3A) and developed a flow cytometry scheme using Trop2 (TACSTD2) as a cell surface marker, given its selectivity for urethral luminal epithelia over Sca-1 (*Ly6a*) in the scRNA-seq data from intact mice (Figure 2C). Trop2 is highly expressed in urethral luminal cells (Figure 2C) and immunostaining for Trop2 overlaps with KRT4 in mouse urethral luminal cells (Figure S4E).

Our hierarchical flow cytometry scheme first separates leukocytes (CD45+), epithelia (CD326+), and stroma (CD45−/CD326−). CD326+ epithelia are then gated into prostate secretory luminal (CD26+), basal (PDPN+) and nonbasal/nonprostate luminal (PDPN−/CD26−) cells (Figure S5A). The previously published cell surface marker CD24 (*Cd24a*) labels prostate luminal cells,[21] but also luminal cells of the ejaculatory ducts and urethra. Hence, we used CD26 (*Dpp4*) which is enriched in prostate luminal epithelia over urethral luminal cells (Figure 2C) to specifically sort out prostate secretory luminal cells. CD26+ prostate luminal cells are enriched in the proximal and distal prostate (42.1% ± 4.8% and 40.1% ± 4.4% of total epithelia, respectively) compared with the urethra (12.5% ± 2.1% of total epithelia). Because basal epithelia express relatively low levels of Trop2 (*Tacstd2*) (Figure 2C), urethral luminal epithelia are more accurately identified in the PDPN−/CD26− (nonbasal/nonprostate luminal) gate. Trop2+ urethral luminal cells represent 20.6% ± 1.6% of total epithelia within the urethral region, and 0.44% ± 0.10% of total epithelia within the proximal prostate, compared with 0.22% ± 0.05% in the distal prostate (from four independent experiments) (Figure 3B and Table S6).

Proximal KRT4+/Sca-1+/NKX3.1− prostate progenitors have been shown to be enriched after castration as well as in tumorigenesis.[22,25,30] To determine whether Trop2+ urethral luminal epithelia are likewise enriched after castration, we used our optimized flow cytometry antibody panel to quantitate epithelial cell types in castrated vs sham-castrated mice. Trop2+ urethral luminal epithelia are increased in prostates from castrated mice (11.9% of total epithelia) compared with sham-castrated mice (1.33% of total epithelia) , while CD26+ prostate luminal epithelia represent 26% of total epithelia in sham-castrated mouse prostates compared with 18% in castrated mice (Figure 3C).

Immunohistochemistry confirms that Trop2 and KRT4 are highly expressed in the proximal ducts (within the skeletal muscle rhabdosphincter surrounding the urethra) compared with the distal prostate lobes (outside the rhabdosphincter) in sham-castrated mice (Figures 3D,E and S6A,B). Trop2+ and KRT4+ luminal cells are increased in the distal prostate lobes after castration (Figure S6C–E). A recent study demonstrated that prostate secretory luminal cells acquire characteristics of urethral luminal (“L2”) cells following castration.[38] Further investigation is required to determine whether the increase in Trop2+/KRT4+ urethral

luminal cells following castration is a consequence of urethral cell expansion or from prostate secretory luminal cells acquiring urethral luminal cell markers.

3.4 | Urethral luminal cells are present during early prostate development in mouse and human

The prostate goes through a developmental process of bud initiation, branching morphogenesis, and canalization.[1,2] Although several adult epithelial cell populations can act as facultative progenitors in tissue regeneration and spheroid assays,[17,41] lineage tracing analyses suggest that the basal and luminal lineages are largely unipotent in the adult.[14,17] However, the transgenes used in these studies (*Krt5* and *Krt8*) label basal and luminal epithelial cells from prostate, urethra, and ejaculatory ducts, highlighting the need for developing tissue-specific markers and understanding when and where they are expressed during prostate development.

To determine whether the identity of urethral luminal epithelia is established early in the developmental process, we examined developmental stages of the mouse and human prostate. Mouse urethral luminal cells could be identified by KRT4 staining during early stages of bud initiation (E18.5) within the urogenital sinus epithelium. Rare KRT4+ cells could be observed in the inner region of prostate buds (Figure 4A). During the branching stage (postnatal day 9, P9), KRT4+ urethral cells were highly concentrated in the urethral epithelium and proximal ducts. KRT4+ cells could also be observed in the distal prostate (Figures 4B and S7). In the adult mouse prostate, KRT4+ urethral cells are restricted to the urethra and urethra-proximal ductal segments and largely absent from the distal glandular region (Figure 4C). In the human male, prostate buds initiate at 10 to 13 weeks and undergo branching morphogenesis beginning at 12 to 18 weeks.[42] At 10- to 12-week gestation, club and hillock urethral luminal cells marked by SCGB1A1 and KRT13, respectively, could be observed in the urethra and developing buds (Figure 4D). Between 19- and 21-week gestation, club and hillock urethral luminal cells could be observed in the urethra and in the proximal segments of branching prostatic ducts (Figures 4E and S7). In the adult human male, club and hillock urethral cells extend into the proximal ductal network as shown in the sagittal plane (Figure 4F). These results demonstrate that the urethral cell types are present during prostate budding and branching morphogenesis, which could have implications for human BPH if urethral luminal epithelia participate as multipotent progenitors during the "embryonic reawakening"[13,43] that has been hypothesized to trigger hyperplastic growth.

3.5 | Urethral luminal epithelia are increased in human BPH and survive 5ARI treatment

BPH is a continuous expansion of the prostate transition zone that affects 70% of men over 70 years old and has been hypothesized to be a reawakening of developmental processes.[12,13] To identify epithelial cell types present in BPH, we performed scRNA-seq on glandular nodules from three patients (dissected away from the urethra) who underwent simple prostatectomy for lower urinary tract symptoms (see Table S1 for clinical data on each patient and Table S3 for sequencing metrics). The epithelia were subclustered for comparison to three young normal prostates[4] (Figures 5A and S1E,F). The results demonstrate an increase in club urethral luminal epithelia from 2% of epithelia in the normal prostate to 9% of epithelia within glandular BPH (Figure 5A). We previously established

PSCA as a highly specific cell surface marker capable of capturing a 94% pure population of urethral luminal cells in humans.[4] To confirm whether PSCA+ urethral luminal cells are increased in glandular BPH in a larger cohort, we performed flow cytometry on nondiseased prostates from young organ donors (n = 6) for comparison to glandular BPH specimens from men (n = 6) undergoing simple prostatectomy (Figure S8 and Table S1). PSCA+ urethral luminal epithelia are significantly increased in glandular BPH compared with normal donor prostates (Figure 5B). With the aggregation of normal and BPH scRNA-seq data, we generated DEGs from each cell type in BPH compared to the same cell type in the normal prostate to get a basic understanding of the functional contributions of each cell type in disease. Table S7 displays the significant DEGs for each epithelial cell type in BPH compared with the same cell type in the normal prostate. To annotate the functional changes in club cells in BPH vs normal human prostate, we performed a Kyoto Encyclopedia of Genes and Genomes (KEGG) analysis[44] of DEGs in BPH club cells compared with club cells from normal healthy donor prostates. Several genes that are significantly upregulated in club cells from BPH tissue compared with club cells from normal prostate tissue belong to immunomodulatory pathways (Figure 5C).

5ARIs are widely used to treat BPH patients. 5ARI treatment shrinks total prostate volume through luminal cell apoptosis by inhibiting the conversion of testosterone to DHT, although this shrinkage is not uniform across the entire gland.[8,10] Given that castration in the mouse enriched for Trop2+/KRT4+ urethral luminal cells (Figures 3C–E and S6), we tested whether urethral luminal cells are increased in areas of atrophy within human BPH in patients treated with a 5ARI. Accordingly, we performed dual immunohistochemistry for club (SCGB1A1) and hillock (KRT13) urethral luminal cells in normal prostates, in men with BPH that were not taking a 5ARI (5ARI-naïve) and men with BPH on 5ARI treatment (Table S1). In normal prostates, club and hillock cells were enriched in the urethra and proximal prostate ducts (Figure 5D). Club and hillock cells were detectable in 5ARI-naïve men with BPH similar to the scRNA-seq data (Figure 5E). However, analysis of prostate sections from 11 different 5ARI-treated men revealed an increase in the number of club and hillock urethral cells in focal areas of atrophy, further suggesting DHT independence of urethral luminal epithelia in areas of prostate luminal cell apoptosis (Figures 5F and S9A,B). Quantification demonstrated that club and hillock staining was significantly higher in 5ARI-treated prostates compared with prostates from untreated (5ARI-naïve) BPH patients (Figure S10).

4 | DISCUSSION

We have produced a cellular anatomy of the mouse prostate and urethral epithelia and compared the molecular identity of equivalent cell types and their locations to the human (Figures 1 and 2). This led to the identification of a mouse urethral luminal cell type that is transcriptionally similar to human urethral cell types identified previously.[4] The mouse urethral luminal cell type is enriched in the epithelium of the urethra as well as proximal prostate ducts that drain into the urethra. We demonstrate that many of the markers previously used to characterize castration-insensitive prostate progenitors in the proximal prostate are highly expressed by urethral luminal cells (Figure 2C).

We performed single-cell analysis separately on preparations of the mouse prostate and urethra and aggregated the data for analysis of common cell types across discrete anatomical regions. We found that a cell population enriched in the urethral cell preparation was also found in the prostate cell preparation. Using immunostaining, we localized this cell type to the luminal layer of the urethra and proximal ducts. We found that luminal cells in the urethral epithelium and a subset of luminal cells in the proximal prostate ducts cluster together *in silico* and are arranged in a continuous array from the urethra up to the transition to prostate secretory epithelium *in situ*. These luminal cells do not express Nkx3.1, a defining feature of prostate luminal cells. Moreover, similar to the human anatomy, mouse urethral luminal cells extend from the urethra into the proximal ducts of the prostate before transitioning to prostate secretory luminal cells (Figure 2A,B). In our own dissections of the mouse prostate lobes away from the urethra, we observe that 0.44% ± 0.10% of the total epithelia in the homeostatic proximal prostate are Trop2+ urethral luminal cells (Table S6), suggesting that urethral luminal cells extend into the proximal ductal network.

After castration, the prostate shrinks due to the loss of prostate secretory luminal cells, but can grow back to its original size with androgen readministration.[18,28] The castration-insensitive cell type that regenerates the prostate has been the subject of considerable research efforts. Cells of the proximal prostate have been shown to display increased castration resistance and regenerative capacity in *in vitro* spheroid assays and tissue regeneration studies.[23,29,30] Although cells from the proximal region of the prostate show increased survival under castrate conditions, subsets of prostate secretory luminal cells can also survive castration.[19,38] Luminal cell populations that are not concentrated in the proximal region, like the castration-resistant Nkx3.1-expressing cells[20] and castration-resistant Bmi1-expressing cells,[45] are capable of contributing to prostate regeneration. A recent study demonstrated that both proximal and distal luminal cells proliferate during prostate regenerative growth, suggesting that prostate growth occurs at several sites instead of in a confined niche.[38] Through scRNA-seq, we have been able show that the urethral luminal cell type expresses several markers like Sca-1,[21,22,29,30] Trop2,[23] LY6D,[24] and KRT4[25,38] that have been used to characterize castration-insensitive proximal prostate progenitors in previous studies. In addition, we observed an enrichment of the Trop2+/KRT4+ urethral luminal cell type after castration. Is the enrichment of urethral cells after castration because of the loss of prostate secretory luminal cells or are urethral cells expanding? A third possibility that was proposed in a recent study was that surviving prostate secretory luminal cells acquire characteristics of urethral luminal cells under conditions of androgen deprivation.[38] Lineage tracing studies of Keratin 4 lineage would answer the question of whether urethral luminal cells in the proximal prostate give rise to prostate secretory luminal epithelium during regenerative growth. The other possibility is that the urethral luminal cells only maintain the pool of urethral cells in the proximal region and prostate secretory luminal cells that survive castration regrow the prostate luminal cell compartment separately.

Our study has revealed the heterogeneity of the urethra and proximal ductal compartment. Urethral luminal cells are present in the epithelium of the urogenital sinus (primitive urethra) during prostate bud initiation. We observed urethral luminal cells in developing prostate buds and proximal branching ducts (Figure 4) and these cells contribute to the proximal

region of the prostate in the adult. Lineage tracing studies using generic luminal Cre drivers like Keratin 8 to label early prostate progenitors have to be reassessed in light of the complexity of the urethra and proximal ductal network. Lineage tracing with Keratin 8 during early prostate development would result in labeling of Keratin 4+ urethral luminal cells from the urogenital sinus as well. The use of urethral luminal-specific Cre drivers will be required to determine whether urethral luminal epithelia of the primitive urogenital sinus can act as a multipotent cell of origin for prostate budding and branching morphogenesis or whether this activity is restricted to multipotent basal epithelia.[14]

The incidence of benign and malignant prostate disease in proximal (transition zone) and distal (peripheral zone) anatomical regions, respectively, has long perplexed prostate biologists.[7,46] It has been proposed that BPH is a reawakening of the morphogenic activity of prostate stromal cells in the per-urethral region which act on prostate progenitors to induce hyperplastic growth.[11,13] However, the full identity of the epithelial cell types that propagate prostate growth has been elusive. Evidence from lineage tracing studies of mitochondrial mutations in humans demonstrates a clonal expansion of cells along the proximal to distal axis from the urethra to the distal prostate in adult men, suggesting that progenitors reside in the proximal region.[26,27] Given the increase in urethral epithelial cells in the prostates of 5ARI-treated men (Figure 5), it is tempting to postulate that BPH is a process of renewed budding and branching from the urethral epithelium. In this scenario, 5ARI treatment acts similar to castration by “trimming the leaves,” that is, removing the DHT-dependent secretory luminal cells and enriching for urethral cell types. Three-dimensional reconstructions of the prostate ductal architecture by emerging techniques like microcomputed tomography will be necessary for confirmation. Another possibility is that surviving secretory luminal cells acquire characteristics of urethral luminal cells, similar to what was observed in the castrated mouse prostate.[38] Further research is required to determine whether BPH involves new ductal outgrowths from the urethra or expansion of existing ducts. Mitochondrial mutations can be used to trace the origin of epithelial cells found within BPH glandular nodules.

Finally, it will be important to characterize the functional role of urethral luminal epithelial cells in maintaining the health of the prostate. Club and hillock epithelia of the lung are anti-inflammatory, antibacterial, and antiviral and can also serve as progenitors under certain conditions.[6,47,48] We have showed previously that club and hillock cells in the prostatic urethra closely resemble their lung counterparts.[4] The transcriptomic signature of urethral epithelial cells also shows immunomodulatory activity, suggesting the potential for a similar functional role in protecting distal prostate tissue from environmental exposures and infections (Figure 5C). The increased abundance of urethral luminal cells within glandular nodules in BPH patients could indicate an expansion in response to infection or inflammation. Alternatively, these cells could be acting as progenitors that differentiate into prostate and contribute to growth due either to intrinsic properties of stemness or extrinsic signaling from the surrounding stroma.[49]

5 | CONCLUSIONS

In this study, we used a combination of scRNA-seq, immunohistochemistry, and flow cytometry to identify the mouse equivalent of human urethral cells which we named urethral luminal cells. These cells extend from the epithelium of the urethra into the proximal prostate lobes and do not express markers of secretory prostate luminal cells. Urethral luminal cells are castration-insensitive and express several markers like Sca-1,[21,22] Trop2,[23] LY6D,[24] and KRT4[25,38] that have been associated with progenitor activity in previous studies. Urethral luminal cells expand in BPH patients, and are able to survive reduced DHT levels following 5ARI treatment. Our results warrant further investigation into the role of urethral cells in human BPH.

Supplementary Material

Refer to Web version on PubMed Central for supplementary material.

ACKNOWLEDGMENTS

We thank the families of organ donors at the Southwest Transplant Alliance for their commitment to basic science research. We acknowledge the assistance of the University of Texas Southwestern Tissue Resource (5P30CA142543), UT Southwestern's Children's Research Institute Flow Cytometry Core and the Whole Brain Microscopy Core. Financial support came from TL1TR002375 and F30DK122686 (HMR), R01DK115477 (DWS); U54DK104310 (DWS and CMV), U01DK110807 and R01DK099328 (CMV); and the generous donations of the Smith, Penson, and Harris families to the UTSW Department of Urology (CGR).

Funding information

Division of Cancer Prevention, National Cancer Institute, Grant/Award Number: 5P30CA142543; National Institute of Diabetes and Digestive and Kidney Diseases, Grant/Award Numbers: F30DK122686, R01DK099328, R01DK115477, TL1TR002375, U01DK110807, U54DK104310

REFERENCES

1. Sugimura Y, Cunha GR, Donjacour AA. Morphogenesis of ductal networks in the mouse prostate. Biol Reprod. 1986;34(5):961–971. [PubMed: 3730488]
2. Thomson AA, Marker PC. Branching morphogenesis in the prostate gland and seminal vesicles. Differentiation. 2006;74(7):382–392. [PubMed: 16916376]
3. Timms BG, Mohs TJ, Didio LJ. Ductal budding and branching patterns in the developing prostate. J Urol. 1994;151(5):1427–1432. [PubMed: 8158800]
4. Henry GH, Malewska A, Joseph DB, et al. A cellular anatomy of the normal adult human prostate and prostatic urethra. Cell Rep. 2018; 25(12):3530–3542.e5. [PubMed: 30566875]
5. Plasschaert LW, Žilionis R, Choo-Wing R, et al. A single-cell atlas of the airway epithelium reveals the CFTR-rich pulmonary ionocyte. Nature. 2018;560(7718):377–381. [PubMed: 30069046]
6. Montoro DT, Haber AL, Biton M, et al. A revised airway epithelial hierarchy includes CFTR-expressing ionocytes. Nature. 2018; 560(7718):319–324. [PubMed: 30069044]
7. McNeal JE. Regional morphology and pathology of the prostate. Am J Clin Pathol. 1968;49(3):347–357. [PubMed: 5645095]
8. Gormley GJ, Stoner E, Bruskewitz RC, et al. The effect of finasteride in men with benign prostatic hyperplasia. The Finasteride Study Group. N Engl J Med. 1992;327(17):1185–1191. [PubMed: 1383816]
9. Platz EA, Joshu CE, Mondul AM, Peskoe SB, Willett WC, Mondul GE. Incidence and progression of lower urinary tract symptoms in a large prospective cohort of United States men. J Urol. 2012;188(2): 496–501. [PubMed: 22704110]

10. Strand DW, Costa DN, Francis F, Ricke WA, Roehrborn CG. Targeting phenotypic heterogeneity in benign prostatic hyperplasia. Differentiation. 2017;96:49–61. [PubMed: 28800482]
11. Isaacs JT. Prostate stem cells and benign prostatic hyperplasia. Prostate. 2008;68(9):1025–1034. [PubMed: 18386293]
12. Isaacs JT, Coffey DS. Etiology and disease process of benign prostatic hyperplasia. Prostate Suppl. 1989;2:33–50. [PubMed: 2482772]
13. McNeal JE. Origin and evolution of benign prostatic enlargement. Invest Urol. 1978;15(4):340–345. [PubMed: 75197]
14. Ousset M, Van Keymeulen A, Bouvencourt G, et al. Multipotent and unipotent progenitors contribute to prostate postnatal development. Nat Cell Biol. 2012;14(11):1131–1138. [PubMed: 23064263]
15. Tika E, Ousset M, Blanpain A, Dannau C. Spatiotemporal regulation of multipotency during prostate development. Development. 2019; 146(20). 10.1242/dev.180224
16. Sugimura Y, Cunha GR, Donjacour AA, Bigsby RM, Brody JR. Whole-mount autoradiography study of DNA synthetic activity during postnatal development and androgen-induced regeneration in the mouse prostate. Biol Reprod. 1986;34(5):985–995. [PubMed: 3730490]
17. Choi N, Zhang B, Zhang L, Ittmann M, Xin L. Adult murine prostate basal and luminal cells are self-sustained lineages that can both serve as targets for prostate cancer initiation. Cancer Cell. 2012;21(2): 253–265. [PubMed: 22340597]
18. Isaacs JT. Control of cell proliferation and death in the normal and neoplastic prostate: a stem cell model In: Rogers CH, Coffey DS, Cunha G, et al., eds. Benign Prostatic Hyperplasia. Bethesda: National Institutes of Health; 1985:85–94.
19. Liu J, Pascal LE, Isharwal S, et al. Regenerated luminal epithelial cells are derived from preexisting luminal epithelial cells in adult mouse prostate. Mol Endocrinol. 2011;25(11):1849–1857. [PubMed: 21940754]
20. Wang X, Julio MK, Economides KD, et al. A luminal epithelial stem cell that is a cell of origin for prostate cancer. Nature. 2009;461(7263): 495–500. [PubMed: 19741607]
21. Kwon OJ, Zhang L, Xin L. Stem cell antigen-1 identifies a distinct androgen-independent murine prostatic luminal cell lineage with bipotent potential. Stem Cells. 2016;34(1):191–202. [PubMed: 26418304]
22. Shi X, Gipp J, Dries M, Bushman W. Prostate progenitor cells proliferate in response to castration. Stem Cell Res. 2014;13(1):154–163. [PubMed: 24905440]
23. Goldstein AS, Lawson DA, Cheng D, Sun W, Garraway IP, Witte ON. Trop2 identifies a subpopulation of murine and human prostate basal cells with stem cell characteristics. Proc Natl Acad Sci U S A. 2008; 105(52):20882–20887. [PubMed: 19088204]
24. Barros-Silva JD, Linn DE, Steiner I, et al. Single-cell analysis identifies LY6D as a marker linking castration-resistant prostate luminal cells to prostate progenitors and cancer. Cell Rep. 2018;25(12):3504–3518.e6. [PubMed: 30566873]
25. Sackmann Sala L, Boutillon F, Menara G, et al. A rare castration-resistant progenitor cell population is highly enriched in Pten-null prostate tumours. J Pathol. 2017;243(1):51–64. [PubMed: 28603917]
26. Moad M, Hannezo E, Buczacki SJ, et al. Multipotent basal stem cells, maintained in localized proximal niches, support directed long-ranging epithelial flows in human prostates. Cell Rep. 2017;20(7):1609–1622. [PubMed: 28813673]
27. Blackwood JK, Williamson SC, Greaves LC, et al. In situ lineage tracking of human prostatic epithelial stem cell fate reveals a common clonal origin for basal and luminal cells. J Pathol. 2011;225(2): 181–188. [PubMed: 21898876]
28. Tsujimura A, Koikawa Y, Salm S, et al. Proximal location of mouse prostate epithelial stem cells: a model of prostatic homeostasis. J Cell Biol. 2002;157(7):1257–1265. [PubMed: 12082083]
29. Burger PE, Xiong X, Coetzee S, et al. Sca-1 expression identifies stem cells in the proximal region of prostatic ducts with high capacity to reconstitute prostatic tissue. Proc Natl Acad Sci U S A. 2005;102(20): 7180–7185. [PubMed: 15899981]

30. Xin L, Lawson DA, Witte ON. The Sca-1 cell surface marker enriches for a prostate-regenerating cell subpopulation that can initiate prostate tumorigenesis. Proc Natl Acad Sci U S A. 2005;102(19):6942–6947. [PubMed: 15860580]
31. Georgas KM, Armstrong J, Keast JR, et al. An illustrated anatomical ontology of the developing mouse lower urogenital tract. Development. 2015;142(10):1893–1908. [PubMed: 25968320]
32. Henry GH, Strand DW, Determining cellular heterogeneity in the human prostate with single cell RNA sequencing; 2018 10.5281/zenodo.2654018
33. Henry GH, Strand DW, Strand Lab analysis of single cell RNA sequencing; 2020 10.5281/zenodo.3687064
34. Strand DW, GUDMAP Consortium; 2020 10.25548/16-WM8C
35. Thielen JL, Volzing KG, Collier LS, Green LE, Largaespada DA, Marker PC. Markers of prostate region-specific epithelial identity define anatomical locations in the mouse prostate that are molecularly similar to human prostate cancers. Differentiation. 2007;75(1): 49–61. [PubMed: 17244021]
36. Kawano N, Araki N, Yoshida K, et al. Seminal vesicle protein SVS2 is required for sperm survival in the uterus. Proc Natl Acad Sci U S A. 2014;111(11):4145–4150. [PubMed: 24591616]
37. Bhatia-Gaur R, Donjacour AA, Sciavolino PJ, et al. Roles for Nkx3.1 in prostate development and cancer. Genes Dev. 1999;13(8):966–977. [PubMed: 10215624]
38. Karthaus WR, Hofree M, Choi D, et al. Regenerative potential of prostate luminal cells revealed by single-cell analysis. Science. 2020; 368(6490):497–505. [PubMed: 32355025]
39. Richardson GD, Robson CN, Lang SH, Neal DE, Maitland NJ, Collins AT. CD133, a novel marker for human prostatic epithelial stem cells. J Cell Sci. 2004;117(Pt 16):3539–3545. [PubMed: 15226377]
40. Hudson DL, Guy AT, Fry P, O'Hare MJ, Watt FM, Masters JR. Epithelial cell differentiation pathways in the human prostate: identification of intermediate phenotypes by keratin expression. J Histochem Cytochem. 2001;49(2):271–278. [PubMed: 11156695]
41. Wang ZA, Mitrofanova A, Bergren SK, et al. Lineage analysis of basal epithelial cells reveals their unexpected plasticity and supports a cell-of-origin model for prostate cancer heterogeneity. Nat Cell Biol. 2013; 15(3):274–283. [PubMed: 23434823]
42. Cunha GR, Vezina CM, Isaacson D, et al. Development of the human prostate. Differentiation. 2018;103:24–45. [PubMed: 30224091]
43. Brennen WN, Isaacs JT. Mesenchymal stem cells and the embryonic reawakening theory of BPH. Nat Rev Urol. 2018;15(11):703–715. [PubMed: 30214054]
44. Kanehisa M, Goto S. KEGG: Kyoto Encyclopedia of Genes and Genomes. Nucleic Acids Res. 2000;28(1):27–30. [PubMed: 10592173]
45. Yoo YA, Roh M, Naseem AF, et al. Bmi1 marks distinct castration-resistant luminal progenitor cells competent for prostate regeneration and tumour initiation. Nat Commun. 2016;7:12943. [PubMed: 27703144]
46. DeMarzo AM, Nelson WG, Isaacs WB, Epstein JI. Pathological and molecular aspects of prostate cancer. Lancet. 2003;361(9361): 955–964. [PubMed: 12648986]
47. Hong KU, Reynolds SD, Giangreco A, Hurley CM, Stripp BR. Clara cell secretory protein-expressing cells of the airway neuroepithelial body microenvironment include a label-retaining subset and are critical for epithelial renewal after progenitor cell depletion. Am J Respir Cell Mol Biol. 2001;24(6):671–681. [PubMed: 11415931]
48. Rawlins EL, Okubo T, Xue Y, et al. The role of Scgb1a1+ Clara cells in the long-term maintenance and repair of lung airway, but not alveolar, epithelium. Cell Stem Cell. 2009;4(6):525–534. [PubMed: 19497281]
49. Wei X, Zhang L, Zhou Z, et al. Spatially restricted stromal wnt signaling restrains prostate epithelial progenitor growth through direct and indirect mechanisms. Cell Stem Cell. 2019;24(5):753–768.e6. [PubMed: 30982770]

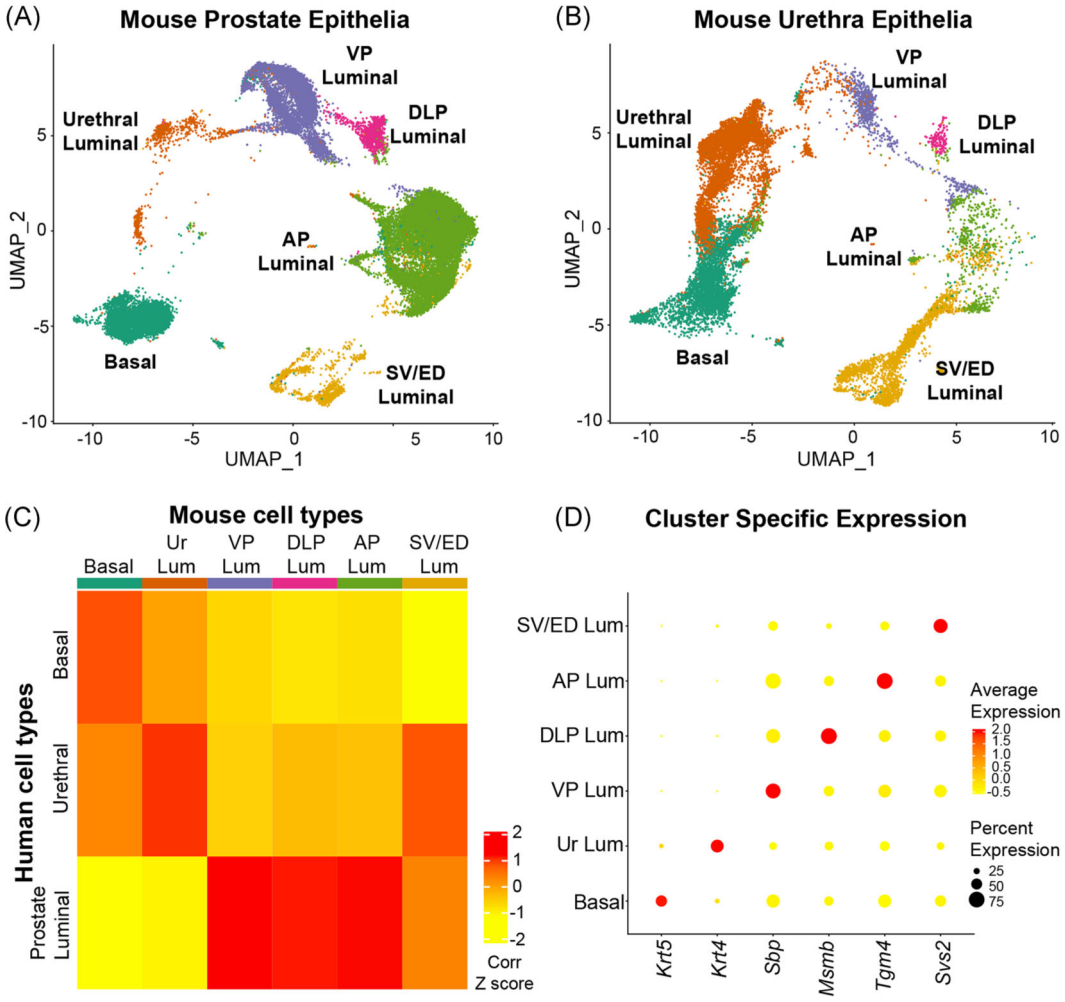

FIGURE 1.

Identification of epithelial cell types of the mouse prostate and prostatic urethra by scRNA-seq. A and B, Mouse prostate lobes ($n = 4$) were dissected away from the rhabdosphincter of the urethra ($n = 3$) and each anatomical region was processed into a single-cell suspension and barcoded separately for scRNA-seq. The data were aggregated and subclustered by epithelial lineage (see Figure S1), and separated into (A) prostate and (B) urethra. C, Statistical correlation of each epithelial cluster of the mouse prostate and urethra with human epithelial cell types. D, Dot plot of differentially expressed genes for each cluster. AP, anterior prostate; DLP, dorsolateral prostate; ED, ejaculatory duct; Lum, luminal; scRNA-seq, single-cell RNA sequencing; SV, seminal vesicle; Ur, urethra; VP, ventral prostate

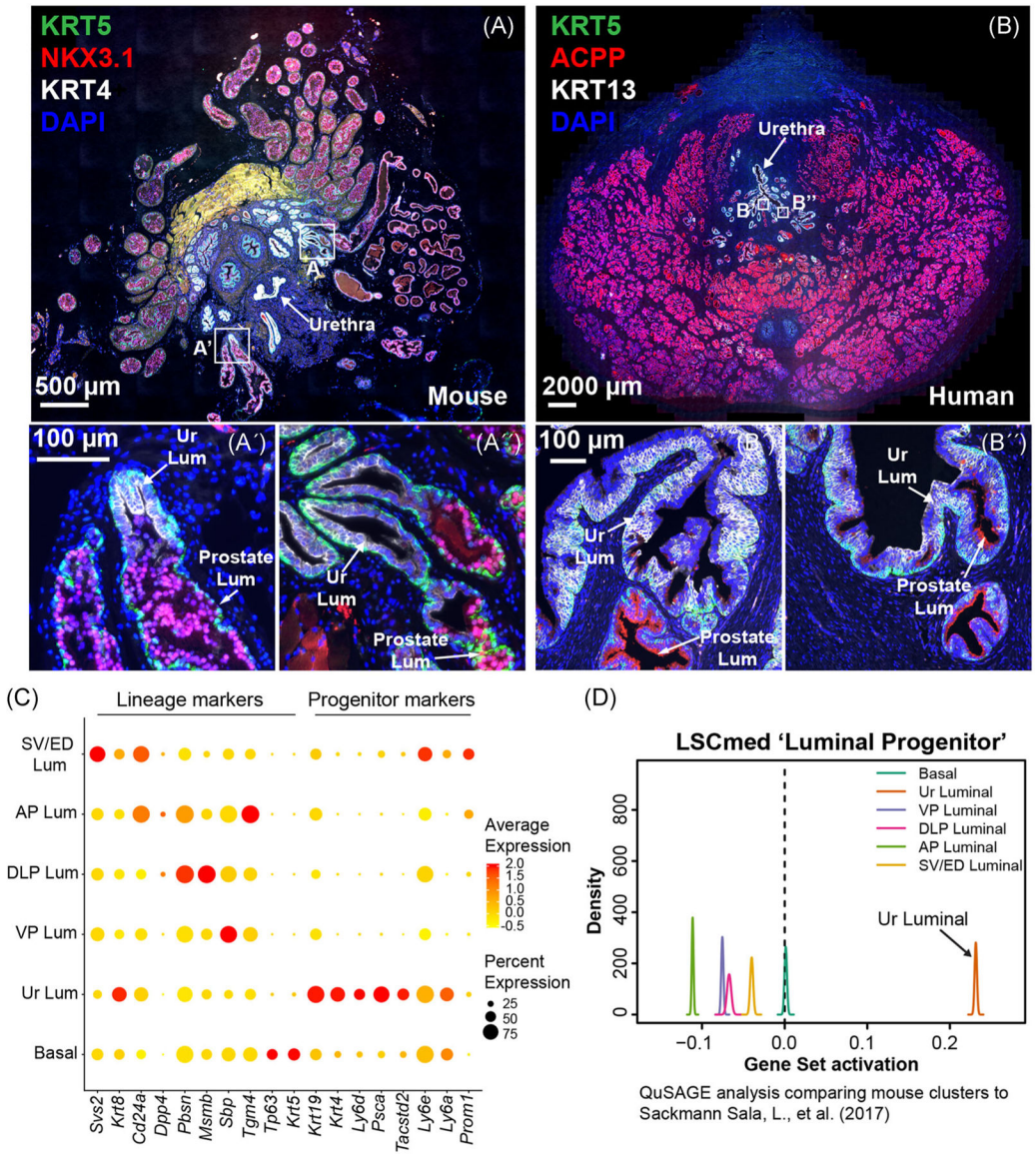

FIGURE 2.

Urethral luminal cells express prostate progenitor markers and extend into the proximal prostate. A, Transverse section through the mouse prostatic urethra labeled with antibodies to KRT4 (in white, labels urethral luminal cells), KRT5 (in green, labels basal cells) and NKX3.1 (in red, labels prostate secretory luminal cells). Magnified insets from (A) are shown in (A′) and (A″). B, Transverse section through a normal human prostate labeled with antibodies to KRT13 (in white, labels hillock urethral cells), KRT5 (in green, labels basal cells) and ACPP (in red, labels prostate secretory luminal cells). Magnified insets from (B) are shown in (B′) and (B″). DAPI staining is shown in blue. C, Dot plot of mouse prostate and urethral epithelial cell type-specific markers and progenitor cell markers. D, Correlation of mouse scRNA-seq clusters to the transcriptomic signature of LSC^{med} "luminal progenitors" from Sackmann Sala et al.[25] AP, anterior prostate; DAPI, 4′,6-diamidino-2-phenylindole; DLP, dorsolateral prostate; ED, ejaculatory duct; Lum, luminal;

scRNA-seq, single-cell RNA sequencing; SV, seminal vesicle; Ur, urethra; VP, ventral prostate

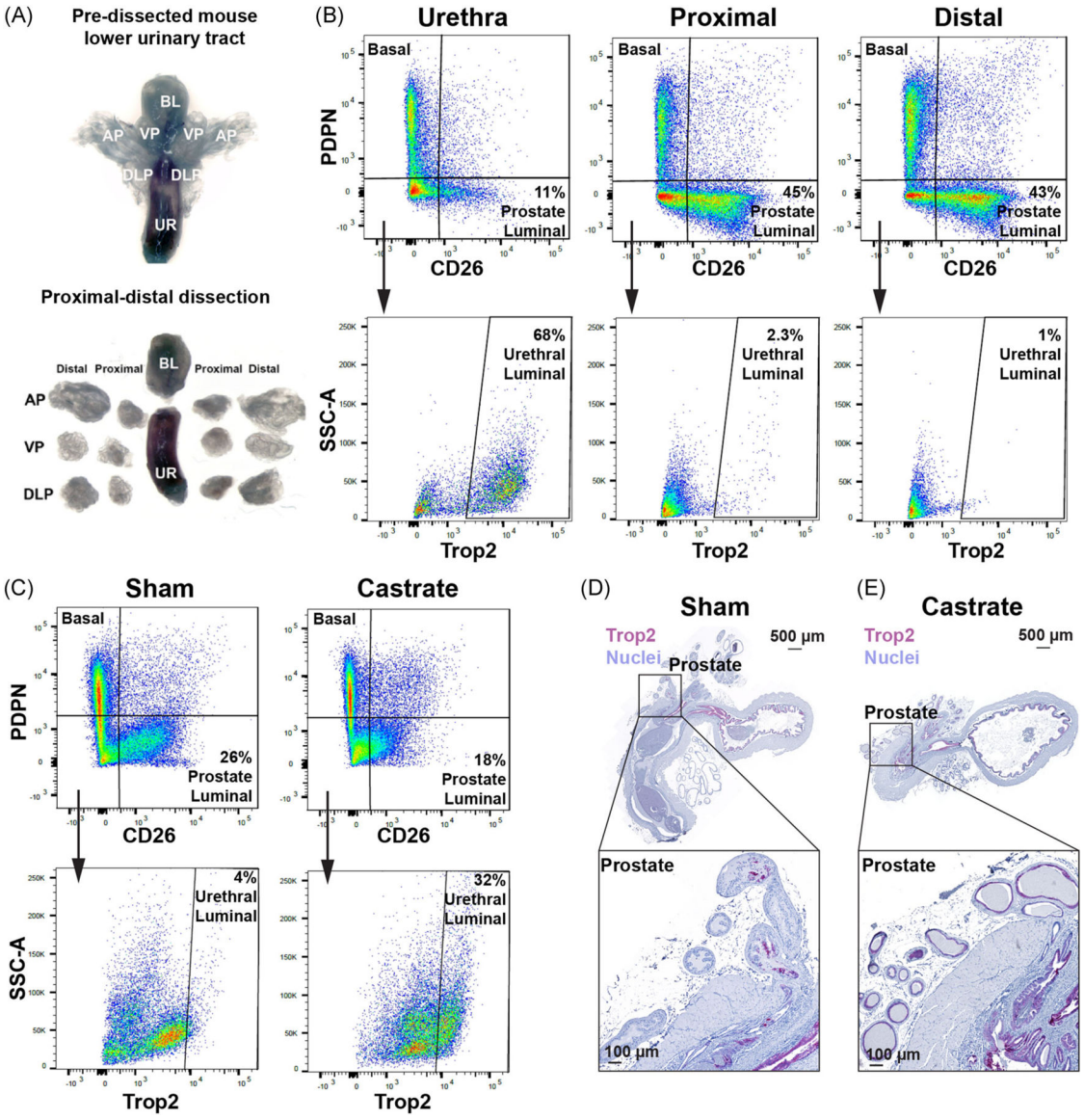

FIGURE 3.

Trop2+ urethral luminal cells are enriched in the prostates of castrated mice. A, Dissection of mouse prostate lobes away from urethra, and into proximal and distal regions. B, Flow cytometry of CD26+ prostate luminal epithelia, PDPN+ basal epithelia, and Trop2+ urethral epithelia in the urethra, proximal prostate, and distal prostate from intact mice. Data are representative of $n = 4$ independent experiments. C, Flow cytometry of Trop2+ urethral luminal cells in prostate tissue from sham-castrated and castrated mice. D and E, Whole-mount lower urinary tract sections from sham-castrated and castrated mice labeled with antibodies to Trop2 (in red) and counterstained with hematoxylin to stain nuclei. Images are representative of $n = 3$ mice per group. AP, anterior prostate; DLP, dorsolateral prostate; VP, ventral prostate

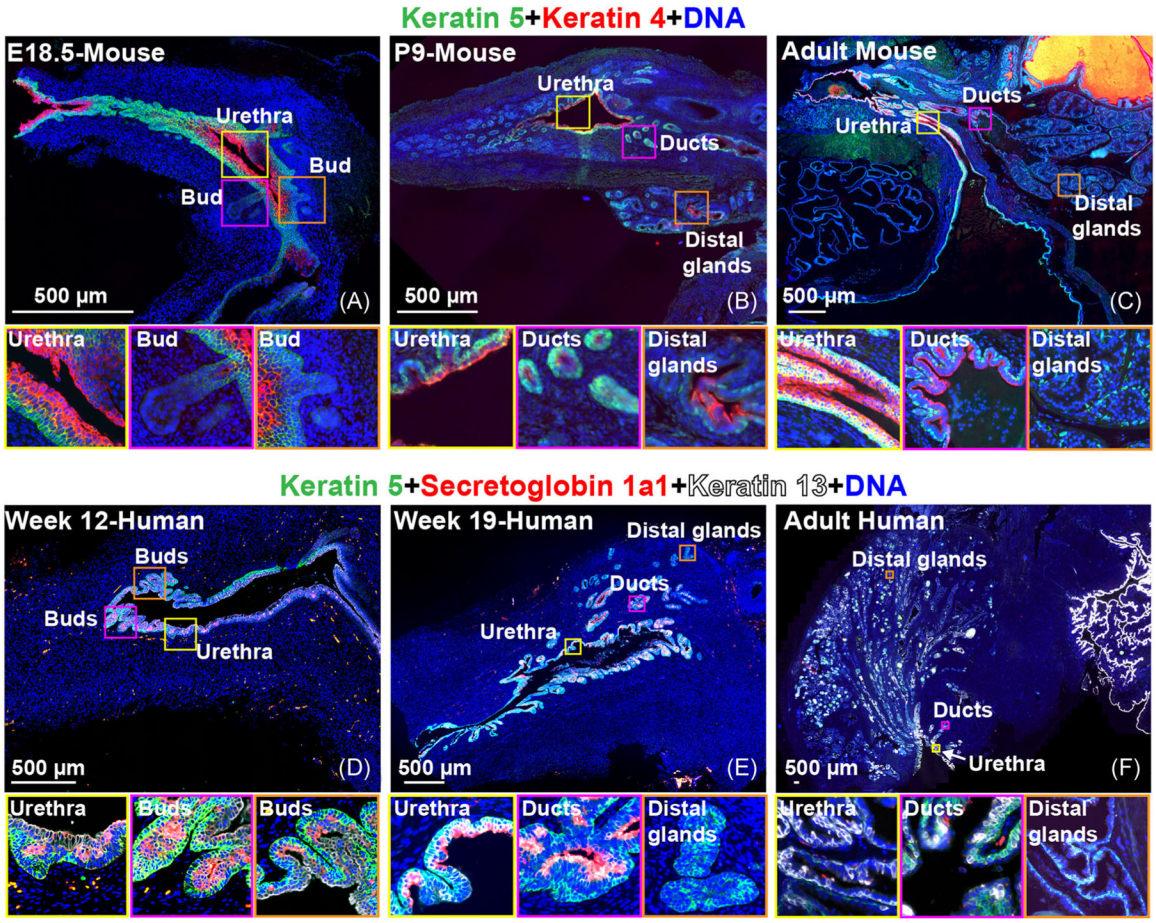

FIGURE 4.

Urethral epithelial identity is established early in prostate development. Mouse lower urinary tract sagittal sections labeled with antibodies to KRT4 (in red, labels urethral luminal cells) and KRT5 (in green, labels basal cells). Stages shown are (A) embryonic day 18.5 (budding), (B) postnatal day 9 (branching), and (C) adult mouse prostate. Human lower urinary tract sagittal sections labeled with antibodies to KRT13 (in white, labels hillock urethral cells), SCGB1A1 (in red, labels club urethral cells), and KRT5 (in green, labels basal cells). Stages shown are (D) 12-week gestation (budding), (E) 19-week gestation (branching), and (F) adult human prostate. DAPI staining is shown in blue. DAPI, 4′,6-diamidino-2-phenylindole

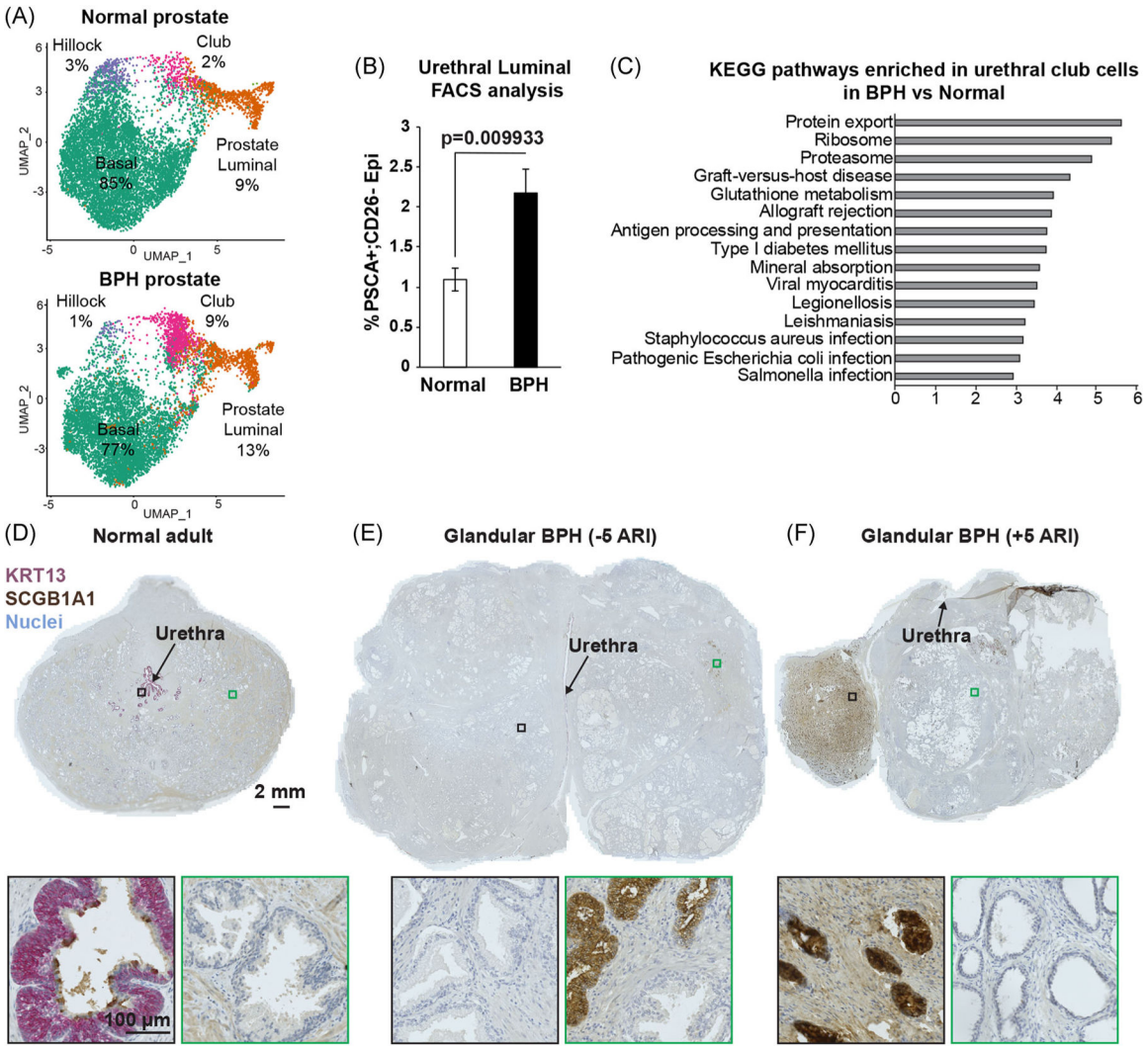

FIGURE 5.

Urethral epithelia are enriched in human BPH and are resistant to 5ARI treatment. A, scRNA-seq of tissue from three patients with glandular BPH demonstrates an enrichment of club epithelia compared with the three young adult normal prostates. B, Quantification of PSCA+ urethral epithelia from normal prostate and BPH prostates by flow cytometry (n = 6 per group). *P* value was obtained from Student's *t* test performed on the two independent groups. C, Fold enrichment of the top 15 KEGG pathways significantly upregulated in club urethral luminal cells from BPH vs normal prostate. D-F, Dual IHC for KRT13 (in red, labels hillock urethral cells) and SCGB1A1 (in brown, labels club urethral cells) on prostate sections from (D) normal adults (n = 5), (E) patients with glandular BPH (n = 10) and (F) 5ARI-treated BPH patients (n = 11). Nuclei were counterstained with hematoxylin. 5ARI, 5-α reductase inhibitor; BPH, benign prostatic hyperplasia; FACS, fluorescence-activated cell sorting; IHC, immunohistochemistry; KEGG, Kyoto Encyclopedia of Genes and Genomes; PSCA, prostate stem cell antigen; scRNA-seq, single-cell RNA sequencing